

# Raman Spectroscopy of $\gamma$ -Si<sub>3</sub>N<sub>4</sub> and $\gamma$ -Ge<sub>3</sub>N<sub>4</sub> Nitride Spinel Phases Formed at High Pressure and High Temperature: Evidence for Defect Formation in Nitride Spinels

Emmanuel Soignard<sup>†</sup> and Paul F. McMillan<sup>\*,†,‡</sup>

Department of Chemistry, Christopher Ingold Laboratories, University College London, 20 Gordon Street, London WC1H 0AJ, U.K., and Davy-Faraday Research Laboratory, Royal Institution of Great Britain, 21 Albemarle Street, London W1X 4BS, U.K.

Received February 9, 2004. Revised Manuscript Received June 15, 2004

The discovery of dense spinel nitride phases,  $\gamma$ -Si<sub>3</sub>N<sub>4</sub> and  $\gamma$ -Ge<sub>3</sub>N<sub>4</sub>, synthesized under high-pressure–high-temperature conditions has resulted in renewed interest in solid-state nitride materials chemistry. The new materials are high hardness ceramics, and they represent a new family of wide band gap semiconductors and optoelectronic materials. The compounds have been characterized by X-ray and electron diffraction and by Raman scattering carried out both on quenched samples and in situ at high pressure in the diamond anvil cell. Here, we assign the Raman-active modes of  $\gamma$ -Si<sub>3</sub>N<sub>4</sub> and  $\gamma$ -Ge<sub>3</sub>N<sub>4</sub> spinels, taking account of impurity phases that can be present within the samples. Laser-heating diamond anvil cell studies carried out at high pressures and at various temperatures lead to the identification of additional Raman features that we assign to the presence of defects, most likely N<sup>3-</sup> vacancies, within the nitride spinels. The intensity of the “defect” peaks varies systematically with the temperature and pressure of synthesis, corresponding to changes in the N<sub>2</sub> activity in equilibrium between the solid nitrides and the surrounding N<sub>2</sub> fluid. The results point the way toward future measurement and control of the defect chemistry achieved within spinel nitrides prepared under high-pressure–high-temperature conditions.

## Introduction

Silicon nitride Si<sub>3</sub>N<sub>4</sub> and the related germanium nitride Ge<sub>3</sub>N<sub>4</sub> are well-known ceramics. Each compound gives rise to two ambient pressure polymorphs ( $\alpha$ -,  $\beta$ -Si<sub>3</sub>N<sub>4</sub>;  $\alpha$ -,  $\beta$ -Ge<sub>3</sub>N<sub>4</sub>), that are constituted by tetrahedrally coordinated SiN<sub>4</sub> or GeN<sub>4</sub> species, connected by trigonal planar or near-planar NSi<sub>3</sub>/NGe<sub>3</sub> groups. The  $\beta$ -polymorph of Si<sub>3</sub>N<sub>4</sub> and Ge<sub>3</sub>N<sub>4</sub> is isomorphic with the silicate minerals phenacite (Be<sub>2</sub>SiO<sub>4</sub>) or willemite (Zn<sub>2</sub>-SiO<sub>4</sub>), and it is usually considered to be the thermodynamically stable form.<sup>1–4</sup> The crystals are hexagonal, with space group *P*6<sub>3</sub>/*m*. The  $\alpha$ -Si<sub>3</sub>N<sub>4</sub>/Ge<sub>3</sub>N<sub>4</sub> polymorphs have a related structure (space group *P*3<sub>1</sub>*c*). These are thought to be metastable at all *P* and *T* conditions; however, they may become stabilized relative to the  $\beta$ -Si<sub>3</sub>N<sub>4</sub>/Ge<sub>3</sub>N<sub>4</sub> polymorphs by incorporation of chemical impurities or defect formation within the structure.<sup>5</sup> Until 1999, all investigations of Si/Ge nitrides had

indicated that the  $\alpha$ - and  $\beta$ -polymorphs of Si<sub>3</sub>N<sub>4</sub> and Ge<sub>3</sub>N<sub>4</sub> were the only polymorphs likely to be encountered over a wide range of temperature and pressure.<sup>6,7</sup>

Recently, during high-pressure–high-temperature experiments carried out independently by groups of Zerr et al. in Germany, and our own research team in Arizona, a new spinel-structured polymorph was reported to exist for each phase ( $\gamma$ -Si<sub>3</sub>N<sub>4</sub>;  $\gamma$ -Ge<sub>3</sub>N<sub>4</sub>), prepared by treating the low-pressure polymorphs or by direct synthesis from the elements under high *P*–*T* conditions.<sup>8–10</sup> The syntheses took place at *P* > 10–12 GPa, and *T* > 1000–1200 °C.  $\gamma$ -Si<sub>3</sub>N<sub>4</sub> and  $\gamma$ -Ge<sub>3</sub>N<sub>4</sub> were also reported to occur as a result of shock-wave treatment of low-pressure Si-nitride polymorphs.<sup>11</sup> In another independent study, a new tetravalent nitride of tin was reported to exist: the new compound Sn<sub>3</sub>N<sub>4</sub> also

\* To whom correspondence should be addressed. E-mail: p.f.mcmillan@ucl.ac.uk.

<sup>†</sup> University College London.

<sup>‡</sup> Royal Institution of Great Britain.

- (1) Popper, P.; Ruddlesden, S. N. *Nature* **1957**, *4570*, 1129.
- (2) Goodman, P.; O'Keeffe, M. *Acta Crystallogr., Sect. B* **1980**, *36*, 2891.
- (3) Borgen, O.; Seip, H. M. *Acta Chem. Scand.* **1961**, *15*, 1789.
- (4) Ruddlesden, S. N.; Popper, P. *Acta Crystallogr.* **1958**, *11*, 465.
- (5) Grün, R. *Acta Crystallogr., Sect. B* **1979**, *35*, 800–804.

(6) Wild, S.; Grieveson, P.; Jack, K. H. *Spec. Ceram.* **1972**, *5*, 385–395.

(7) Riedel, R. *Handbook of Ceramic Hard Materials*, 1st ed.; Wiley-VCH: New York, 2000.

(8) Zerr, A.; Miehe, G.; Serghiou, G.; Schwarz, M.; Kroke, E.; Riedel, R.; Fuess, H.; Kroll, P.; Boehler, R. *Nature* **1999**, *400*, 340.

(9) Leinenweber, K.; O'Keeffe, M.; Somayazulu, M.; Hubert, H.; McMillan, P. F.; Wolf, G. W. *Chem.-Eur. J.* **1999**, *5*, 3076.

(10) Serghiou, G.; Miehe, G.; Tschauner, O.; Zerr, A.; Boehler, R. *J. Chem. Phys.* **1999**, *111*, 4659.

(11) Sekine, T.; He, H.; Kobayashi, T.; Zhang, M.; Xu, F. *Appl. Phys. Lett.* **2000**, *76*, 3706–3708.

had the spinel structure, and it was prepared by chemical precursor techniques at ambient pressure conditions.<sup>12</sup> The spinel-structured polymorphs contain the group 14 elements in both 4- and 6-coordinated sites. This was only the second reported occurrence of octahedral coordination to nitrogen for Si,<sup>13</sup> and it still remains the only report of octahedral GeN<sub>6</sub> chemistry to date. The new dense nitrides exhibit low compressibility and high hardness values, and they could yield a new family of useful materials for cutting and grinding applications.<sup>7,14,15</sup> Theoretical calculations as well as preliminary experimental studies also indicate that they represent a new class of wide band gap nitride materials,<sup>8,16–19</sup> with optoelectronic characteristics that might be comparable to those of the wurtzite-structured (Ga, Al, In)N compounds, that are currently being developed as a technologically important family of blue/green-UV solid-state light-emitting diodes and lasers.<sup>20,21</sup>

Early studies of  $\gamma$ -Si<sub>3</sub>N<sub>4</sub> and  $\gamma$ -Ge<sub>3</sub>N<sub>4</sub> nitride spinels used Raman scattering spectroscopy to identify and characterize the new compounds, along with powder X-ray and electron diffraction of quenched materials.<sup>8,10,22</sup> Here, we present a detailed assignment of the Raman peaks of  $\gamma$ -Si<sub>3</sub>N<sub>4</sub> and  $\gamma$ -Ge<sub>3</sub>N<sub>4</sub>, and we identify features that do not form part of the expected spectra for the spinel-structured phases. In particular, certain "additional" spectral features are assigned to the presence of defects within the nitride spinel structures that we believe are associated with N<sup>3-</sup> vacancies. These assignments are based on previous results for oxide spinels that are known to contain O<sup>2-</sup> vacancies, along with consideration of the behavior of the peak intensities during high  $P$ - $T$  synthesis and annealing conditions for the nitride spinels.

It is well-known that spinel-structured oxides can contain vacancies on cation and/or anion sites, and that the presence of such defects greatly influences their electronic, optical, and mechanical properties.<sup>23</sup> It is thus important to develop methods to identify, characterize, and control the solid-state defect chemistry of spinel-structured nitrides. The presence of defects that may be present at minor concentrations is not easy to establish by chemical analysis or diffraction techniques. However, even small concentrations of defects can give rise to readily observable features in the Raman spectra of spinel-structured compounds, and this technique has been successfully applied in studies of defects in oxide spinels.<sup>24–28</sup> Our results obtained here will help establish Raman spectroscopy as a technique for observing,

characterizing, and controlling the defect chemistry within nitride spinels, as a function of their synthesis and processing conditions.

## Experimental Section

$\gamma$ -Si<sub>3</sub>N<sub>4</sub> and  $\gamma$ -Ge<sub>3</sub>N<sub>4</sub> spinels were prepared by laser-heated diamond anvil cell (LH-DAC) or multi-anvil high-pressure-high-temperature (HP-HT) synthesis methods, using  $\alpha$ -,  $\beta$ -structured Si<sub>3</sub>N<sub>4</sub>/Ge<sub>3</sub>N<sub>4</sub> (Aldrich 99.99% chemical purity), or elemental Ge/Si (Aldrich 99.999%) as starting materials, loaded with pure N<sub>2</sub> as a pressure-transmitting/reactant medium.<sup>8,9,14,29</sup> All starting materials were stored under N<sub>2</sub> or Ar prior to use; care was taken during loading to eliminate or minimize interaction of O<sub>2</sub> or H<sub>2</sub>O with the sample during synthesis. Ge<sub>3</sub>N<sub>4</sub> as obtained from the manufacturer usually contains an approximately 1:2 mixture of  $\alpha$ -/ $\beta$ -polymorphs. For certain syntheses, Ge<sub>3</sub>N<sub>4</sub> samples were first treated at  $P = 9$  GPa and  $T = 900$  °C to obtain pure  $\beta$ -Ge<sub>3</sub>N<sub>4</sub> for use in synthesis experiments (we note that the  $P$ ,  $T$  conditions were incorrectly reported in the previous work; the correct values are given here).<sup>22,29,30</sup> Ge<sub>3</sub>N<sub>4</sub> samples supplied commercially also often contain up to ~1% elemental Ge as a crystalline or amorphous impurity phase, that gives rise to a weak peak at ~300 cm<sup>-1</sup> (crystalline Ge) or to broad features in the 150–300 cm<sup>-1</sup> region (amorphous Ge);<sup>22</sup> such Ge impurities are not usually detectable by X-ray diffraction.

The multi-anvil sample of Si<sub>3</sub>N<sub>4</sub> was synthesized under high  $P$ - $T$  conditions using a Walker type cylindrical multi-anvil press using a Fei-type 8/3 assembly contained inside 8 tungsten carbide cubes. The assembly was pressurized to oil pressures of 5000 psi (520 tonnes), corresponding to a maximum pressure developed within the samples of ~23 GPa. The sample was resistively heated to  $T = 2000$  °C for 2 h. The starting material used in the experiment was  $\alpha$ -Si<sub>3</sub>N<sub>4</sub>. The sample was loaded into a graphite capsule to provide a reducing atmosphere at high  $P$ - $T$ , surrounded by Re foil that acts as the furnace material. The Re furnace is surrounded by a LaCrO<sub>3</sub> sleeve, placed inside a MgAl<sub>2</sub>O<sub>4</sub>/MgO octahedron of pressure-transmitting material. Temperatures were recorded using a type C thermocouple placed next to the sample. The structural nature of the sample after quench/recovery was determined by powder X-ray diffraction (Siemens D5000). The chemical composition of the sample was investigated using electron microprobe analysis: it was determined to have an oxygen content below the detection limit of the equipment, less than 3 atomic %.

For LH-DAC synthesis experiments, powdered samples were pressed into pellets a few micrometers thick, and then loaded cryogenically with N<sub>2</sub> under O<sub>2</sub>/H<sub>2</sub>O-free conditions into a 130  $\mu$ m diameter hole that had been electro-eroded into a stainless steel or Re gasket, pre-indented to a thickness of ~30  $\mu$ m. Samples were then subjected to pressures ranging from 8.5 to 30 GPa, for laser-heating experiments and HP-HT synthesis runs. Pressures were generally measured via the ruby fluorescence technique.<sup>31</sup> In some cases, the calibrated shift of solid N<sub>2</sub> Raman peaks was also used to estimate synthesis pressures. To initiate high  $P$ - $T$  syntheses or phase transformations, samples were heated using a 100 W multi-

(12) Scotti, N.; Kockelmann, W.; Senker, J.; Traβel, S.; Jacobs, H. *Z. Anorg. Allg. Chem.* **1999**, *625*, 1435.

(13) Köllisch, K.; Schnick, W. *Angew. Chem., Int. Ed.* **1999**, *38*, 357–359.

(14) Soignard, E.; Somayazulu, M.; Dong, J.; Sankey, O. F.; McMillan, P. F. *J. Phys.: Condens. Matter* **2001**, *13*, 557.

(15) Zerr, A.; Kempf, M.; Schwarz, M.; Krobe, E.; Göken, M.; Riedel, R. *J. Am. Ceram. Soc.* **2002**, *85*, 86–90.

(16) Kroll, P. *J. Solid State Chem.* **2003**, *176*, 530–537.

(17) Dong, J.; Sankey, O. F.; Deb, S. K.; McMillan, P. F. *Phys. Rev. B* **2000**, *61*, 11979.

(18) Dong, J.; Deslippe, J.; Sankey, O. F.; Soignard, E.; McMillan, P. F. *Phys. Rev. B* **2003**, *67*, 094104.

(19) McMillan, P. F. *Nat. Mater.* **2002**, *1*, 19–25.

(20) Nakamura, S. *Semicond. Semimet.* **1997**, *48*, 391–443.

(21) Ponce, F. A.; Bour, D. P. *Nature* **1997**, *386*, 351–359.

(22) Deb, S. K.; Dong, J.; Hubert, H.; McMillan, P. F.; Sankey, O. F. *Solid State Commun.* **2000**, *114*, 137.

(23) Wells, A. F. *Structural Inorganic Chemistry*, 5th ed.; Oxford University Press: New York, 1984.

(24) White, W. B.; DeAngelis, B. A. *Spectrochim. Acta* **1967**, *23A*, 985–995.

(25) O'Horo, M. P.; Frisillo, A. L.; White, W. B. *J. Phys. Chem. Solids* **1973**, *34*, 23–28.

(26) Ishii, M.; Hiraishi, J.; Yamanaka, T. *Phys. Chem. Miner.* **1982**, *8*, 64–68.

(27) Fraas, L. M.; Moore, J. E.; Salzberg, J. B. *J. Chem. Phys.* **1973**, *58*, 3585.

(28) McMillan, P.; Akaogi, M. *Am. Mineral.* **1987**, *72*, 361–364.

(29) Somayazulu, M. S.; Leinenweber, K.; Hubert, H.; McMillan, P. F.; Wolf, G. W. In *AIRAPT-17*; Manghnani, M. H., Nellis, H., Nicol, M. F., Eds.; University Press: Hyderabad, India, 1999; pp 663–666.

(30) McMillan, P. F.; Deb, S. K.; Dong, J. *J. Raman Spectrosc.* **2003**, *34*, 567–577.

(31) Mao, H. K.; Xu, J.; Bell, P. M. *J. Geophys. Res.* **1986**, *91*, 4673–4676.

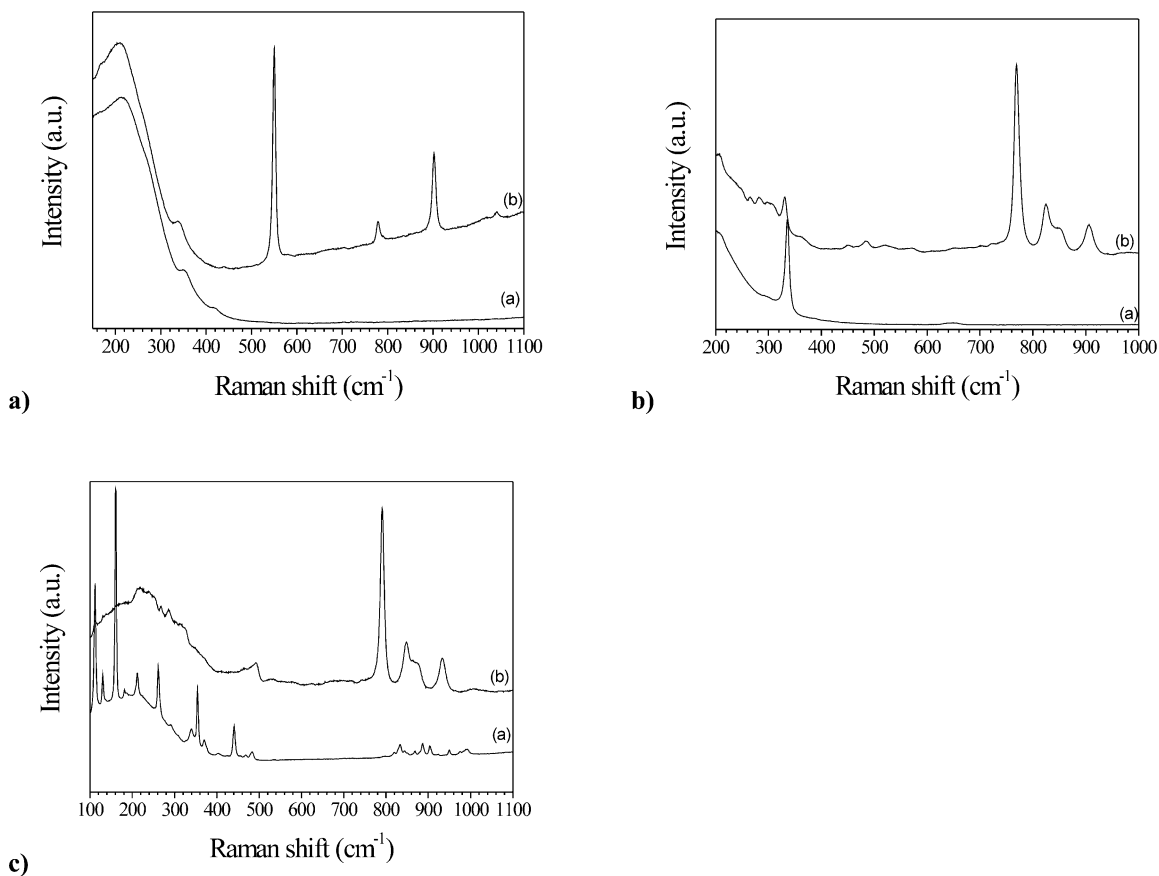


**Figure 1.** (a) Raman spectrum of a mixture of Si + N<sub>2</sub> loaded in the diamond anvil cell at 16.5 GPa (below), and spectrum of  $\gamma$ -Si<sub>3</sub>N<sub>4</sub> spinel obtained after laser heating (above). The broad band at low frequency is due to the nitrogen pressure medium. (b) Raman spectrum of a mixture of Ge + N<sub>2</sub> in the diamond anvil cell at 10.5 GPa (below), and spectrum of  $\gamma$ -Ge<sub>3</sub>N<sub>4</sub> spinel obtained after laser heating (above). The high-frequency region contains “extra” peaks that are assigned to the presence of defects (N<sup>3-</sup>vacancies): see text. (c) Raman spectrum of germanium nitride (mainly  $\beta$ -Ge<sub>3</sub>N<sub>4</sub>, along with a small amount of  $\alpha$ -Ge<sub>3</sub>N<sub>4</sub>) loaded into the diamond anvil cell in N<sub>2</sub> at 16.7 GPa (below), and spectrum after laser heating, showing formation of  $\gamma$ -Ge<sub>3</sub>N<sub>4</sub> spinel (above).

mode Nd<sup>3+</sup>:YAG laser or a 50 W single-mode CO<sub>2</sub> laser. The YAG laser was split into two beams and focused on the sample from both sides of the cell, using optically matched Mitutoyo long working distance microscope objectives. The CO<sub>2</sub> laser was focused on one side of the sample using a ZnSe lens. The temperatures during the LH-DAC experiments were determined by thermal emission spectrometry: synthesis temperatures ranged between 1500 and 3000 K.<sup>32–35</sup> The results of typical LH-DAC synthesis runs from the elements or low-pressure polymorphs are shown in Figure 1.

The ruby fluorescence, thermal emission, and Raman scattering spectra were analyzed using a custom-built micro-focus optical spectroscopy system installed at UCL<sup>36</sup> (Figure 2). The Raman scattering and ruby luminescence were excited either with an air-cooled 50 mW Ar<sup>+</sup> laser ( $\lambda_0 = 514.5; 488.0$  nm) or a 35 mW He–Ne laser ( $\lambda_0 = 632.8$  nm), focused into the DAC using a Mitutoyo 50SL objective with a focal length of 20.5 mm. The Raman scattered signals were collected in backscattered geometry through the same objective. Kaiser SuperNotch filters were placed in the optical path to discriminate the laser

line from the Raman scattering. Optical spectroscopy was carried out using a 500 mm focal length Acton 300 spectrometer and a liquid N<sub>2</sub>-cooled back-illuminated silicon CCD detector.

## Results and Discussion

### Raman Spectra of $\gamma$ -Ge<sub>3</sub>N<sub>4</sub> and $\gamma$ -Si<sub>3</sub>N<sub>4</sub> Spinels.

From symmetry analysis, five Raman-active modes are expected to occur for the spinel structure:

$$\Gamma_{\text{optic(R)}} = 3T_{2g} + 1E_g + 1A_{1g} \quad (1)$$

In particular, two modes with A<sub>1g</sub> + T<sub>2g</sub> symmetry are expected to occur in the high-frequency region, that are derived from  $\nu_1$  (A<sub>1</sub>) and  $\nu_3$  (T<sub>2</sub>) symmetric and anti-symmetric stretching vibrations of tetrahedral SiN<sub>4</sub>/GeN<sub>4</sub> groups. Features at lower wavenumber correspond to tetrahedral deformation modes, coupled with stretching/bending vibrations associated with octahedral (SiN<sub>6</sub>/GeN<sub>6</sub>) sites.

A typical Raman spectrum of a  $\gamma$ -Ge<sub>3</sub>N<sub>4</sub> sample synthesized at high  $P$ – $T$  in a multi-anvil device and recovered to ambient  $P$ – $T$  conditions is shown in Figure 3a. In the high-frequency region associated with tetrahedral Ge–N stretching vibrations, the strong peak at 729 cm<sup>-1</sup> is readily assigned to the asymmetric (T<sub>2g</sub>) stretching mode, consistent with Deb et al.<sup>22</sup> These

(32) Saxena, S. K.; Dubrovinsky, L. S. *3rd NIRIM International Symposium on Advanced Materials (ISAM '96)*; National Institute for Research in Inorganic Materials: Tsukuba, Japan, 1996; p 137.

(33) Jeanloz, R.; Kavner, A. *Philos. Trans. R. Soc. London, Ser. A* **1996**, *354*, 1279.

(34) Jephcoat, A.; Besedin, S. P. *Philos. Trans. R. Soc. London, Ser. A* **1996**, *354*, 1333.

(35) Shen, G.; Mao, H. K.; Hemley, R. J. *3rd NIRIM International Symposium on Advanced Materials (ISAM '96)*; National Institute for Research in Inorganic Materials: Tsukuba, Japan, 1996; p 149.

(36) Soignard, E. *Chemistry*; University College London: London, 2003; p 176.

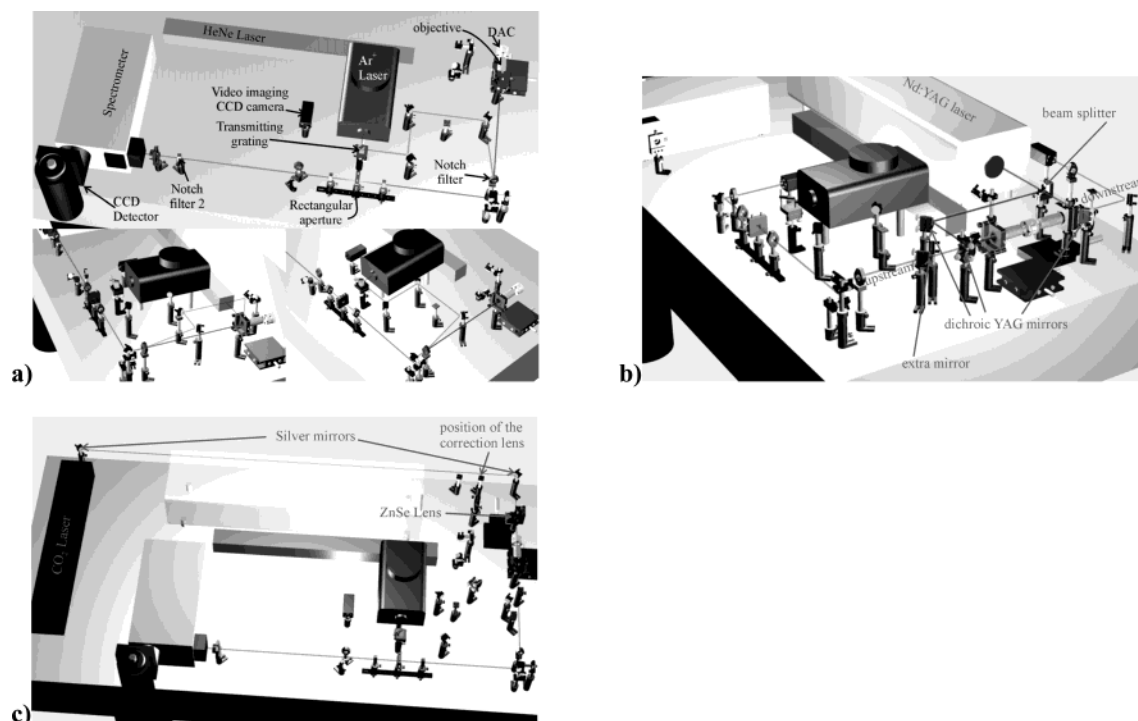


**Figure 2.** (a) The Raman scattering/laser-heating DAC laboratory installed at UCL. Raman spectra are excited with blue-green lines of an Ar<sup>+</sup> laser or red lines of a He–Ne laser, using a Kaiser notch filter to steer the beam into the sample. Signals are collected in a backscattering geometry via a Mitutoyo long working distance objective followed by a variable aperture spatial filter and are sent into an Acton 500i spectrograph. The Kaiser filter used in the transmission mode discriminates between the incident laser light and Raman scattered signals. Signals are detected using a LN<sub>2</sub>-cooled back-illuminated Princeton Instruments CCD. The same optical path is used to measure the ruby fluorescence to determine pressure, and also to observe thermal emission to measure temperature via gray-body fits to the Planck function. (b) For certain materials, especially dark-colored compounds such as the Ge<sub>3</sub>N<sub>4</sub> samples used in this study and metals, it is convenient to use Nd<sup>3+</sup>:YAG laser heating ( $\lambda_0 = 1064$  nm) for synthesis reactions under HP–HT conditions in the DAC. A 100 W laser beam is split into two paths and focused into the cell from each side using a matched pair of objectives. (c) Other samples, including many oxides and Si<sub>3</sub>N<sub>4</sub> studied here, do not couple well to the near-IR radiation provided by the Nd<sup>3+</sup>:YAG beam. For these samples, we use a 50 W CO<sub>2</sub> laser ( $\lambda_0 = 10$   $\mu$ m) for heating. The laser beam is focused into the cell from a single side using a ZnSe lens.

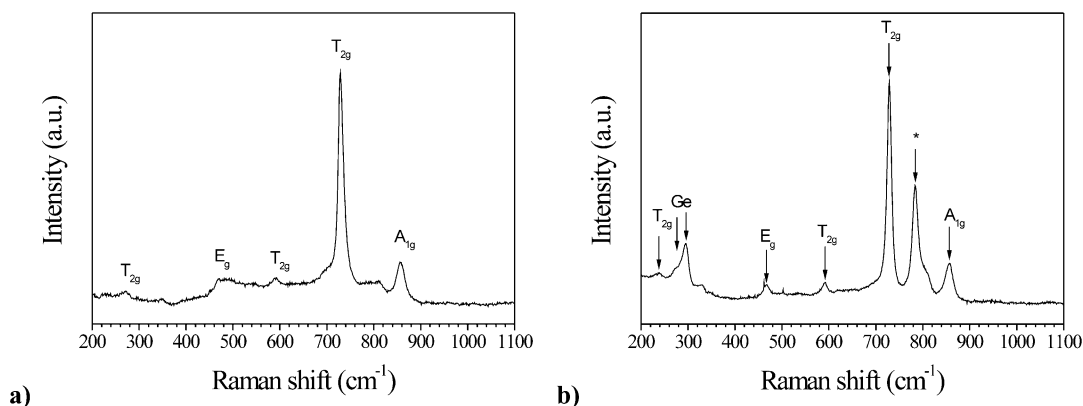


**Figure 3.** (a) Raman spectrum of an aliquot of the  $\gamma$ -Ge<sub>3</sub>N<sub>4</sub> sample previously studied by Deb et al.,<sup>22</sup> recovered from a multi-anvil synthesis run at 12 GPa and 1200–1400 K.<sup>9</sup> In the previous study, a peak was present at 300–320 cm<sup>-1</sup>, that was assigned to the lowest frequency mode expected for  $\gamma$ -Ge<sub>3</sub>N<sub>4</sub>. That peak does not appear in the present spectrum: it is assigned to elemental Ge that was present as an impurity in the sample. (b) Raman spectrum obtained at room pressure and temperature for a sample of spinel-structured  $\gamma$ -Ge<sub>3</sub>N<sub>4</sub> spinel synthesized from Ge + N<sub>2</sub> at 18 GPa and 1500 K using laser heating in a diamond anvil cell, showing the “extra” doublet of peaks in the high-frequency region, that we assign to the presence of N<sup>3-</sup> vacancies within the sample (see text).

authors also observed that the peak at 856 cm<sup>-1</sup> was extinguished under cross-polarized conditions (“HV” spectra), and so it was assigned to the symmetric (A<sub>1g</sub>) GeN<sub>4</sub> stretching vibration. This assignment is in excellent agreement with the results of ab initio density functional calculations carried out within the local density approximation (LDA)<sup>16,17</sup> (Table 1).

Deb et al.<sup>22</sup> also noted the appearance of additional features lying between these two assigned peaks, for most spectra. These “extra” modes often took the form of a doublet, with maxima at  $\sim 770$  and  $\sim 820$  cm<sup>-1</sup>. In the spectrum shown in Figure 3a, this “additional” doublet is barely visible. However, its intensity is highly variable among samples;<sup>22</sup> for example, it is present



**Table 1. Raman Peak Positions for  $\gamma$ -Si<sub>3</sub>N<sub>4</sub> and  $\gamma$ -Ge<sub>3</sub>N<sub>4</sub><sup>a</sup>**

	$\gamma$ -Si <sub>3</sub> N <sub>4</sub> expt: this study	$\gamma$ -Si <sub>3</sub> N <sub>4</sub> theor: Kroll <sup>16</sup>	$\gamma$ -Si <sub>3</sub> N <sub>4</sub> theor: Fang <sup>41</sup>	$\gamma$ -Ge <sub>3</sub> N <sub>4</sub> expt: this study, MA	$\gamma$ -Ge <sub>3</sub> N <sub>4</sub> expt: this study, DAC	$\gamma$ -Ge <sub>3</sub> N <sub>4</sub> expt: Deb <sup>22</sup>	$\gamma$ -Ge <sub>3</sub> N <sub>4</sub> theor: Kroll <sup>16</sup>	$\gamma$ -Ge <sub>3</sub> N <sub>4</sub> theor: Dong <sup>17</sup>
T <sub>2g</sub>		413	415	230; 270; 324?	300; 319?	??	244	245
E <sub>g</sub>	519	518	522	469	465	472	471	467
T <sub>2g</sub>	729	500	726	591	587	593	574	576
T <sub>2g</sub>	840	838	840	729	725	730	719	710
A <sub>g</sub>	975	946	972	856	850	858	831	830

<sup>a</sup>  $\gamma$ -Si<sub>3</sub>N<sub>4</sub>: Experimental values from this study, and from LDA calculations of P. Kroll<sup>16</sup> and C. M. Fang et al.<sup>41</sup>  $\gamma$ -Ge<sub>3</sub>N<sub>4</sub>: Experimental values from this study, for samples synthesized in the multi-anvil device (MA) and laser-heated diamond cell (DAC) and recovered to ambient conditions, as compared to peak positions determined by S. K. Deb et al.,<sup>22</sup> and to calculated values from LDA/GGA calculations of P. Kroll<sup>16</sup> and J. Dong et al.<sup>17</sup>

with an intensity equal to that of the A<sub>1g</sub> mode in the spectrum of the LH-DAC sample that was shown in Figure 1c, and it is observed with even greater intensity in Figure 3b. The origin of this feature is discussed below.

In the lower frequency region, weak peaks at 591 and 469 cm<sup>-1</sup> were assigned by Deb et al. to the T<sub>2g</sub> and E<sub>g</sub> modes associated with GeN<sub>4</sub> deformation vibrations, coupled with GeN<sub>6</sub> stretching/bending contributions. Once more, there is excellent agreement between the observed and calculated peak frequencies<sup>16,22</sup> (Table 1). The lowest frequency T<sub>2g</sub> mode is predicted to occur at 245 cm<sup>-1</sup>; however, experimental assignment of this mode is still not yet certain. Deb et al. observed a depolarized feature at ~320 cm<sup>-1</sup> that they suggested could be assigned to the T<sub>2g</sub> vibration of  $\gamma$ -Ge<sub>3</sub>N<sub>4</sub>. We observed a similar peak at 307 cm<sup>-1</sup> in most of the samples prepared by multi-anvil synthesis in this study (Figure 3a). However, many spectra, including some taken from aliquots of the same sample studied by Deb et al., showed no evidence for this peak (Figure 3b). We now believe that this feature should be assigned to elemental germanium that is present as an impurity within the samples. The zone center T<sub>2g</sub> phonon of bulk Ge occurs at 298 cm<sup>-1</sup>. This feature is observed within commercial Ge<sub>3</sub>N<sub>4</sub> samples used as precursors for high-pressure experiments.<sup>22,30</sup> The Raman peak frequency, width, and line shape of semiconductors such as Ge and Si are known to be functions of the particle size and any strains present within the crystals.<sup>37,38</sup> During compression, Ge contained as an impurity within the sample transforms to the  $\beta$ -Sn phase. Like Si, it reverts to one or more metastable tetrahedral forms during decompression, rather than going directly to the stable diamond-structured polymorph.<sup>39</sup> Alternatively, elemental Ge can be produced in situ by reaction at high pressure, or by thermal or laser-induced decomposition of decompressed samples at ambient conditions, that can give rise to micro- to nanoscale impurity particles or strained materials with shifted and broadened lines. In our study, it was observed that increasing the laser power generally caused an irreversible increase in the intensity of the ~300 cm<sup>-1</sup> peak. We suggest that this

is due to the occurrence of the decomposition reaction 2:



The spectra of various samples recovered from multi-anvil and LH-DAC syntheses also contain weak unassigned peaks at 230, 273, and in the 320–350 cm<sup>-1</sup> region, any of which could correspond to the “missing” T<sub>2g</sub> vibration of  $\gamma$ -Ge<sub>3</sub>N<sub>4</sub> spinel (Deb et al.,<sup>22</sup> Figure 3). Finally, there is a very weak peak occurring at 520 cm<sup>-1</sup> in all of the spectra of  $\gamma$ -Ge<sub>3</sub>N<sub>4</sub> samples that has not yet been assigned (Figure 3).

In Figure 4, we show the unpolarized Raman spectrum of a polycrystalline sample of  $\gamma$ -Si<sub>3</sub>N<sub>4</sub> spinel prepared by multi-anvil high *P*–*T* synthesis (Figure 4a), as well as parallel (“VV”)– and perpendicular (“VH”)–polarized spectra obtained from samples synthesized by LH-DAC techniques from elemental Si + N<sub>2</sub>, after recovery to ambient *P*–*T* conditions (Figure 4b). The spectra are dominated by two sharp, intense peaks at 519 and 840 cm<sup>-1</sup>. From the results of our polarized study, the high-frequency peak is readily assigned to the T<sub>2g</sub> asymmetric stretching mode of SiN<sub>4</sub> units. There is a weaker polarized peak at 985 cm<sup>-1</sup> that we can assign to the corresponding symmetric A<sub>1g</sub> stretching vibration. The calculated frequencies for these two modes are 838 and 946 cm<sup>-1</sup>, respectively<sup>16</sup> (Table 1). There is also an additional weak feature at 1065 cm<sup>-1</sup> that is apparent in the spectrum of the multi-anvil sample (Figure 4a), which has not yet been assigned (Figure 4). Certain samples synthesized at high temperature in the LH-DAC also show additional features in the high-frequency region; these are described and discussed below. The sharp, strong peak at 519 cm<sup>-1</sup> is assigned to the E<sub>g</sub> deformation vibration of SiN<sub>4</sub> groups (also SiN<sub>6</sub> stretching/bending) that was calculated at 518 cm<sup>-1</sup> (Table 1): it is much more intense than the corresponding mode for  $\gamma$ -Ge<sub>3</sub>N<sub>4</sub>. It is worth noting that this peak overlaps with the Raman mode of diamond-structured elemental Si, which could be present as an impurity within the samples, by analogy with Ge nitrides, as discussed above.

Identification of the second T<sub>2g</sub> mode of  $\gamma$ -Si<sub>3</sub>N<sub>4</sub> is difficult. This vibration was predicted to occur at 500 cm<sup>-1</sup>,<sup>16</sup> causing it to be obscured by the strong E<sub>g</sub> peak (Figure 4). The corresponding mode of  $\gamma$ -Ge<sub>3</sub>N<sub>4</sub> was identified at 591 cm<sup>-1</sup>, as compared to calculated values of 574/576 cm<sup>-1</sup><sup>16,17</sup> (Table 1). Weak features do appear in  $\gamma$ -Si<sub>3</sub>N<sub>4</sub> spectra at ~560 cm<sup>-1</sup>, or ~490 cm<sup>-1</sup>, that is,

(37) Kolobov, A. V. *J. Mater. Sci.: Mater. Electron.* **2004**, *12*, 195–203.

(38) Deb, S. K.; Wilding, M.; Somayazulu, M.; McMillan, P. F. *Nature* **2001**, *414*, 528.

(39) Liu, L.-g.; Bassett, W. A. *Elements, Oxides, Silicates: High-Pressure Phases with Implications for the Earth's Interior*; Oxford University Press: New York, 1986.

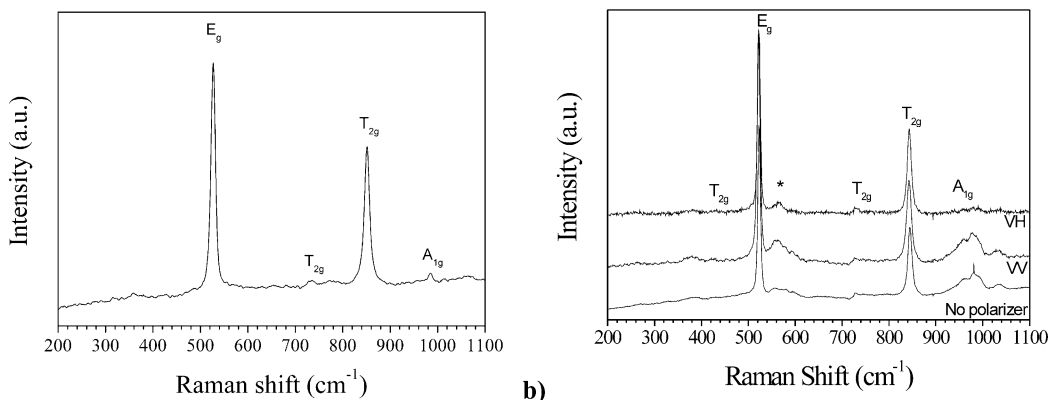


**Figure 4.** (a) Unpolarized Raman spectrum of a polycrystalline  $\gamma$ - $\text{Si}_3\text{N}_4$  sample recorded at room pressure following high-pressure–high-temperature synthesis at 23 GPa and 2300–2600 K in a multi-anvil device.<sup>40</sup> (b) Unpolarized (bottom) and parallel (“VV”) and perpendicular (“VH”) polarized spectra of polycrystalline  $\gamma$ - $\text{Si}_3\text{N}_4$  recorded at room pressure for a sample synthesized in the laser-heated DAC at 16 GPa and 1500 K. Peak symmetry assignments were made by comparison with ab initio (LDA) calculations, and from systematic variations in peak positions within a  $\gamma$ -(Si,Ge) $_3\text{N}_4$  spinel nitride solid solution.<sup>40</sup>

in the high- or low-frequency tail of the strong  $E_g$  mode; however, their appearance is not consistent between spectra (Figure 4). From a recent study of systematic variations in structural parameters and Raman peak positions among spinel-structured  $\text{Si}_3\text{N}_4$ – $\text{Ge}_3\text{N}_4$  solid solutions, we also have preliminary indications that the  $T_{2g}$  mode might even occur in 700–750  $\text{cm}^{-1}$  range for  $\gamma$ - $\text{Si}_3\text{N}_4$ .<sup>40</sup> In all of the present spectra, a weak peak occurs at 729  $\text{cm}^{-1}$  for decompressed samples, which could be assigned to the second  $T_{2g}$  vibration (Figure 4). This peak position matches very well with a recent calculation by Fang et al.<sup>41</sup> Fang et al. calculated the second  $T_{2g}$  vibration to occur at 726  $\text{cm}^{-1}$ .

Finally, identification and assignment of the lowest frequency  $T_{2g}$  vibration is also problematic, as was already found to be the case for  $\gamma$ - $\text{Ge}_3\text{N}_4$ . This mode is predicted to occur at 413  $\text{cm}^{-1}$ .<sup>16</sup> There is no obvious feature at this position in the spectra of any of the decompressed samples (Figure 4). A very subtle “bump” can just be discerned at 420–430  $\text{cm}^{-1}$  upon close examination of the data; however, there is also a very weak broad band with its maximum at  $\sim 360$   $\text{cm}^{-1}$ . Either of these features could correspond to the predicted third  $T_{2g}$  mode of  $\gamma$ - $\text{Si}_3\text{N}_4$ .

In the assignment of modes associated with  $\gamma$ - $\text{Ge}_3\text{N}_4$  and  $\gamma$ - $\text{Si}_3\text{N}_4$ , it was often found useful to track the peaks observed immediately following high  $P$ – $T$  synthesis in the LH-DAC back to ambient conditions. Pressure shifts ( $\partial\nu_j/\partial P$ ) for vibrational modes of  $\gamma$ - $\text{Ge}_3\text{N}_4$  and  $\gamma$ - $\text{Si}_3\text{N}_4$  are shown in Figure 5, and these are listed in Table 2, along with calculated mode Grüneisen parameters

$$\gamma_j = -\frac{\partial \ln \nu_j}{\partial \ln V} = -\frac{V \partial \nu_j}{\nu_j \partial V} \quad (3)$$

using the measured  $P = 1$  atm volume ( $V_0$ ) and bulk modulus values ( $K_0 = 1/V_0 \partial V/\partial P$ : 295 and 308 GPa for  $\gamma$ - $\text{Ge}_3\text{N}_4$  and  $\gamma$ - $\text{Si}_3\text{N}_4$ , respectively<sup>14,29</sup>). This was particularly important in the determination of features associated with the elemental semiconductors Ge and Si, which could be present either as unreacted materials

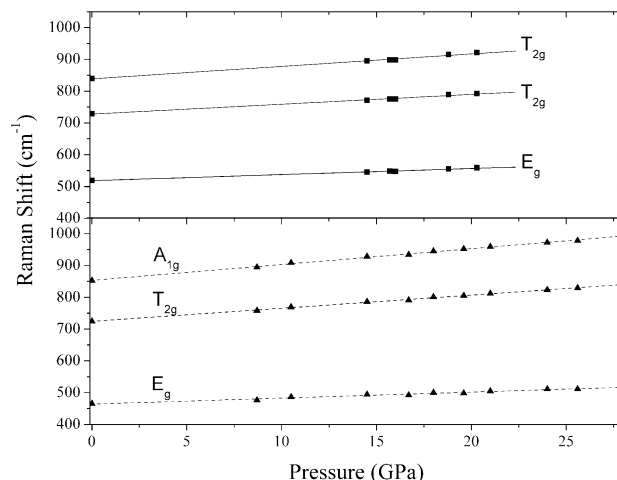


**Figure 5.** Raman shift as a function of pressure for selected Raman peaks for  $\gamma$ - $\text{Ge}_3\text{N}_4$  ( $\blacktriangle$ ) and  $\gamma$ - $\text{Si}_3\text{N}_4$  ( $\blacksquare$ ). The data were collected from several experiments.

**Table 2. Pressure Shifts and Mode Grüneisen Parameters for Raman-Active Vibrations of  $\gamma$ - $\text{Si}_3\text{N}_4$  and  $\gamma$ - $\text{Ge}_3\text{N}_4$**

	$\gamma$ - $\text{Si}_3\text{N}_4$ $\nu_i$	$\gamma$ - $\text{Si}_3\text{N}_4$ $\partial\nu_i/\partial P$	$\gamma$ - $\text{Si}_3\text{N}_4$ $\gamma_{i0}$	$\gamma$ - $\text{Ge}_3\text{N}_4$ $\nu_i$	$\gamma$ - $\text{Ge}_3\text{N}_4$ $\partial\nu_i/\partial P$	$\gamma$ - $\text{Ge}_3\text{N}_4$ $\gamma_{i0}$
$T_{2g}$				300–320?		
$E_g$	519	−1.39	1.27	465	−1.22	1.45
$T_{2g}$	729	−2.24	1.46	587		
$T_{2g}$	840	−2.85	1.61	725	−2.68	2.05
$A_g$	975			850	−3.23	2.10

or as impurities resulting from decomposition reactions, within the samples. The high-pressure forms ( $P > 8$ – $10$  GPa) of these materials are metallic phases (e.g., with the  $\beta$ -Sn) structure, with very weak but characteristic Raman peaks.<sup>42,43</sup> These then back-transformed upon decompression to give rise to the strong Raman features associated with stable diamond-structured or metastable tetrahedral/nanostructured materials, giving rise to, for example, peaks for elemental Ge at 300–320  $\text{cm}^{-1}$ , observed for the recovered samples. For example, in Figure 1b, we show the Raman spectrum of a Ge +  $\text{N}_2$  sample prior to laser heating at 10.5 GPa that

(40) Soignard, E.; McMillan, P. F.; Leinenweber, K., in preparation.

(41) Fang, C. M.; de Wijs, G. A.; Hintzen, H. T.; de With, G. J. *Appl. Phys.* **2003**, *93*, 5175–5180.

(42) Olijnyk, H. *Phys. Rev. Lett.* **1992**, *68*, 2232–2234.

(43) Olijnyk, H.; Jephcoat, A. P. *Phys. Status Solidi B—Basic Res.* **1999**, *211*, 413–420.

contains a single strong peak at  $318\text{ cm}^{-1}$  due to elemental diamond-structured Ge that has not yet undergone its transformation into the metallic  $\beta$ -Sn structured phase, which occurs near this pressure.<sup>39</sup> In the case of the Si + N<sub>2</sub> example shown in Figure 1a, by pressurization to  $P = 16.5\text{ GPa}$ , the semiconducting element has already undergone its diamond/ $\beta$ -Sn phase transition, and only very weak bands due to metallic high-density polymorphs of Si are observed at  $\sim 100$  and  $\sim 400\text{ cm}^{-1}$ .<sup>42</sup> Similar peaks due to the  $\beta$ -Sn form of elemental Ge are also clearly observed in spectra taken at high pressure in the DAC from samples of  $\beta$ -Ge<sub>3</sub>N<sub>4</sub> at  $P = 16.7$  and  $10.5\text{ GPa}$ , following laser-heating syntheses (Figure 1c).

Making mode assignments for  $\gamma$ -Si<sub>3</sub>N<sub>4</sub> and  $\gamma$ -Ge<sub>3</sub>N<sub>4</sub> in the low-frequency regime at high pressure in the DAC is complicated by the presence of strongly Raman-active lattice vibrational modes from the N<sub>2</sub> pressure medium<sup>44–48</sup> (Figure 1). The high-pressure polymorphism in solid N<sub>2</sub> is well-studied, but it is still under investigation.<sup>44,46,49,50</sup> At ambient  $T$ , the fluid pressure medium first solidifies into the *hcp*  $\beta$ -N<sub>2</sub> phase at  $1.7\text{ GPa}$ , which then recrystallizes into a cubic (*Pm3n*) polymorph “ $\delta$ -N<sub>2</sub>” at  $4.9\text{ GPa}$ . A second-order transition occurs into the recently described “ $\delta_{loc}$ ” polymorph at  $P \approx 11\text{ GPa}$ , and then a further transformation occurs into rhombohedral ( $R\bar{3}c$ )  $\epsilon$ -N<sub>2</sub> at  $P = 17.5\text{ GPa}$ .<sup>44,49,50</sup> A further phase transition into  $\zeta$ -N<sub>2</sub> occurs above  $P = 25\text{ GPa}$ ; however, this transition lies above the synthesis pressure range of our experiments. For most of the synthesis experiments carried out here, the N<sub>2</sub> pressure medium was present in its solid  $\delta$  ( $\delta_{loc}$ ) form, before and after laser heating.

**“Extra” Peaks in the Raman Spectra of  $\gamma$ -Ge<sub>3</sub>N<sub>4</sub> and  $\gamma$ -Si<sub>3</sub>N<sub>4</sub> Spinel Nitrides: Evidence for Defect Formation.** It has been noted that “extra” peaks often appear in the high-frequency region for  $\gamma$ -Ge<sub>3</sub>N<sub>4</sub>, which usually take the form of a doublet with maxima at  $\sim 770$  and  $\sim 820\text{ cm}^{-1}$ . These additional features that occur within the tetrahedral Ge–N stretching region are particularly apparent in the spectra of samples synthesized by laser heating at high temperatures from Ge + N<sub>2</sub>, in the DAC synthesis experiments (Figure 1b). However, they are also present, with variable intensity within and between samples, in spectra of samples prepared in multi-anvil syntheses and recovered to ambient conditions (e.g., Figure 3, ref 22).

From symmetry analysis, only two Raman-active modes are expected in the high-frequency tetrahedral stretching region, for either “normal” or “inverse” spinels.<sup>24,25</sup> Any additional features in the region must be due to (a) the presence of impurity phases, or (b) the occurrence of defects, such as disorder or the presence

of vacancies on cation or anion vacancies, within the spinels. These would result in the appearance of new Raman features due to the lowering of the local symmetry around the tetrahedral sites, through breakdown of the  $k = 0$  selection rule, and/or the appearance of new vibrational modes due to the presence of, for example, 3-coordinated (Si,Ge)- or N-centered species associated with the vacancy sites. The symmetry implications of such possibilities for the vibrational spectra of spinel-structured compounds was discussed by White and O'Horo.<sup>24,25</sup>

In the case of nominally stoichiometric oxide spinels, for example, MgAl<sub>2</sub>O<sub>4</sub>, analogous “additional” features are also often observed to be present in the high-frequency stretching region.<sup>24–26</sup> Within a “normal” MgAl<sub>2</sub>O<sub>4</sub> spinel, Mg<sup>2+</sup> cations occupy tetrahedral sites and Al<sup>3+</sup> ions are octahedral. However, most Mg–Al spinels exhibit some degree of mixed “normal-inverse” structure, in which some of the Al<sup>3+</sup> ions occupy tetrahedral sites. The normal-inverse ratio is a sensitive function of the  $P$ – $T$  synthesis conditions and quench/decompression conditions.<sup>51,52</sup> The appearance of the “extra” high-frequency Raman peaks can be interpreted in this case as due to cation disorder, in which Al<sup>3+</sup> ions that are present within tetrahedral sites in the “inverse spinel” structure (i.e., <sup>IV</sup>Al<sup>VI</sup>(MgAl)O<sub>4</sub> vs <sup>IV</sup>Mg<sup>VI</sup>Al<sub>2</sub>O<sub>4</sub>) give rise to additional AlO<sub>4</sub> breathing vibrations that are observed in the Raman spectrum. Spinel containing a single metal atom such as magnetite (Fe<sub>3</sub>O<sub>4</sub>) can also exhibit “normal” versus “inverse” structure due to the ordering of Fe<sup>2+</sup>/Fe<sup>3+</sup> cations on octahedral and tetrahedral sites. However,  $\gamma$ -Ge<sub>3</sub>N<sub>4</sub> and  $\gamma$ -Si<sub>3</sub>N<sub>4</sub> spinels contain only a single type of cation and have an oxidation state of +4 on both octahedral and tetrahedral sites, so neither of these mechanisms can operate. However, “additional” Raman features also appear within the high-frequency TO<sub>4</sub> stretching region of spectra of nonstoichiometric MgAl<sub>2</sub>O<sub>4</sub>–Al<sub>2</sub>O<sub>3</sub> spinels, which contain vacancies on both cation and anion sites.<sup>24–26,53,54</sup> In this case, the “extra” high-frequency modes are associated with the presence of O<sup>2–</sup> vacancies, which give rise to TO<sub>3</sub> sites within the spinel structure. In the case of  $\gamma$ -Ge<sub>3</sub>N<sub>4</sub>, we follow the same assignment for the nonstoichiometric oxide spinels, and we propose that the additional high-frequency features are due to GeN<sub>3</sub> sites resulting from the formation of N<sup>3–</sup> vacancies within the structure.

It might be argued that the additional Raman features could possibly be due to the presence of impurity phase(s). No other high-pressure phases have been observed to occur experimentally within the Ge<sub>3</sub>N<sub>4</sub> system. Other GeN<sub>4</sub>-containing phases that have been proposed to exist include olivine and willemite-II structures.<sup>16,17</sup> However, based on the predicted spectra, neither of these structures could give rise to the “extra” peaks observed; either the frequencies do not match, or else whole series of other peaks should be observed. Also, ab initio calculations of the relative stabilities

(44) Bini, R.; Ulivi, L.; Kreutz, J.; Jodl, H. J. *J. Chem. Phys.* **2000**, *112*, 8522–8529.

(45) Hemley, R. J.; Mao, H. K. *J. Low Temp. Phys.* **2001**, *122*, 331–344.

(46) Gregoryanz, E.; Goncharov, A. F.; Hemley, R. J.; Mao, H. K.; Somayazulu, M.; Shen, G. Y. *Phys. Rev. B* **2002**, *66*, 224108.

(47) LeSar, R.; Ekberg, S. A.; Jones, L. H.; Mills, R. L.; Schwalbe, L. A.; Schiferl, D. *Solid State Commun.* **1979**, *32*, 131–134.

(48) Olijnyk, H.; Daufer, H.; Rubly, M.; Jodl, H. J.; Hochheimer, H. D. *J. Chem. Phys.* **1990**, *93*, 45–54.

(49) Hanfland, M.; Lorenzen, M.; Wassilew-Reul, C.; Zontone, F. *Rev. High-Pressure Sci. Technol.* **1998**, *7*, 787–789.

(50) Hellwig, H.; Daniels, W. B.; Hemley, R. J.; Mao, H. K.; Gregoryanz, E.; Yu, Z. H. *J. Chem. Phys.* **2001**, *115*, 10876–10882.

(51) Wood, B. J.; Kirkpatrick, R. J.; Montez, B. *Am. Mineral.* **1986**, *71*, 999–1006.

(52) Navrotsky, A. *Phys. Chem. Miner.* **1984**, *10*, 192–193.

(53) de Wijs, G. A.; Fang, C. M.; Kresse, G.; de With, G. *Phys. Rev. B* **2002**, *65*, 094305.

(54) Cynn, H.; Sharma, S. K.; Cooney, T. F.; Nicol, M. *Phys. Rev. B* **1992**, *45*, 500–502.



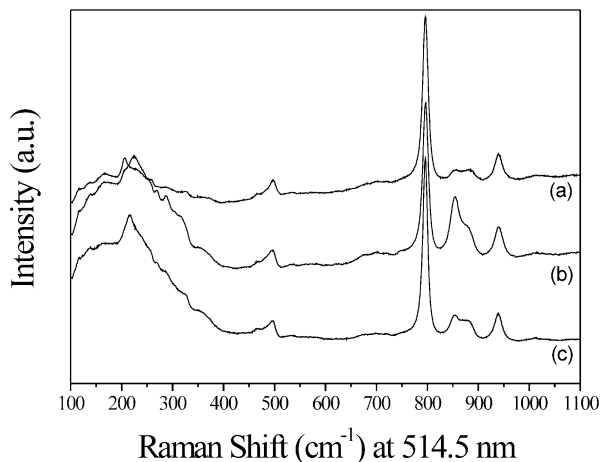
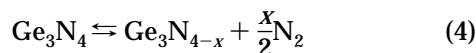


**Figure 6.** Raman spectra of  $\gamma$ - $\text{Ge}_3\text{N}_4$  spinel (a) after synthesis in the diamond anvil cell at 18 GPa and 1700 K from Ge in a  $\text{N}_2$  medium, (b) following reheating in the cell at 2500 K, and (c) following reannealing at 1700 K under the same conditions.

( $E(V)$  curves) indicate that formation of other high-density  $\text{Ge}_x\text{N}_y$  compounds is unlikely to occur during the high  $P$ - $T$  synthesis conditions used here.<sup>8,16,17</sup> We conclude the “extra” peaks are due to  $\text{N}^{3-}$  defect formation within the high  $P$ - $T$  synthesis reactions, in equilibrium between the solid phase and the  $\text{N}_2$  pressure medium.

Such  $\text{N}^{3-}$  vacancies would be formed during high  $P$ - $T$  syntheses by reaction between  $\gamma$ - $\text{Ge}_3\text{N}_4$  and the surrounding nitrogen fluid medium, according to the equilibrium:



We tested this hypothesis by carrying out controlled laser-heating experiments at various temperatures in situ at high pressures (Figure 6). We had already observed qualitatively that the intensity of the “defect” doublet tended to increase with increasing temperature of synthesis, and to decrease for higher synthesis pressure, when the spectra were measured in situ in the DAC following synthesis. In Figure 6, we show spectra for a  $\gamma$ - $\text{Ge}_3\text{N}_4$  spinel sample that was (a) synthesized at 18 GPa and 1700 K, then (b) annealed at 2500 K while maintained within the cell at the same pressure surrounded by the  $\text{N}_2$  fluid environment, then (c) reannealed at 1700 K. The intensity of the high-frequency doublet that we assign to the presence of  $\text{N}^{3-}$  vacancy defects within the nitride spinel structure is obviously reversible, suggesting reestablishment of an equilibrium associated with reaction 3 as a function of the temperature at a given pressure.

From our data, we cannot yet evaluate the relationships between the possible  $\text{N}^{3-}$  vacancy concentrations and the resulting intensity of the “extra” Raman peaks. From work to date on stoichiometric  $\gamma$ - $\text{Ge}_3\text{N}_4$  and  $\gamma$ - $\text{Si}_3\text{N}_4$  spinels, the relative intensities of Raman peaks due to different types of vibrations (e.g., stretching vs bending modes) cannot be readily understood or predicted reliably: for example, the overall appearance of the spectra of the two group 14 nitrides is quite dissimilar (e.g., Figures 3, 4). Because we do not yet fully understand the matrix elements for Raman scattering

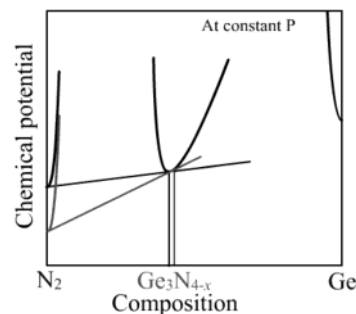


**Figure 7.** Schematic Gibbs' free energy (chemical potential,  $\mu$ ) versus composition ( $X$ ) diagram relevant to formation of  $\gamma$ - $\text{Ge}_3\text{N}_{4-x}$  spinels in the Ge- $\text{N}_2$  system. At all temperatures where spinel is stable, the  $\mu$ - $X$  curve for  $\text{Ge}_3\text{N}_4$  lies below that for Ge +  $\text{N}_2$ . The composition of the nitride spinel (i.e.,  $x$  in  $\text{Ge}_3\text{N}_{4-x}$ ) is determined by the common tangent with the component with which the spinel phase is in equilibrium: in the case of LH-DAC experiments, the  $\text{N}_2$  end-member. The chemical potential for  $\text{N}_2$  fluid decreases more rapidly than that for the solid phases with increased  $T$ , so the common tangent encounters the  $\text{Ge}_3\text{N}_{4-x}$  composition at larger values of  $x$ ; that is,  $\text{N}^{3-}$  vacancies are created within the spinel.

associated with vibrations of the ideal structures, we cannot estimate the contributions from vibrations around postulated vacancy sites, not the degree of Raman activity that might be activated by removing the  $q = 0$  selection rule by defect formation. We have carried out series of chemical analyses using electron microprobe techniques for samples recovered from the high  $P$ - $T$  synthesis experiments (both multi-anvil and LH-DAC), and we have not been able to detect any significant nitrogen loss from the nitride spinel compositions. However, such analyses do not determine light element concentrations well (i.e., no better than a few percent relative concentration), and careful analysis of future samples recovered from a statistically significant range of high  $P$ - $T$  syntheses will be required to test and establish the correlations between spinel stoichiometries and the Raman “defect” peak intensities. It is worth noting that such correlations have still not been established at all for the corresponding oxide spinels, which have been studied intensively for many years now, despite the technological importance of these materials, and for which the presence of  $\text{O}^{2-}$  vacancy-related high-frequency Raman peaks is well established in the literature.<sup>24–26</sup>

We could understand the thermodynamics of formation of  $\text{N}^{3-}$  vacancies within  $\gamma$ - $\text{Ge}_3\text{N}_{4-x}$  spinels under high  $P$ - $T$  conditions by construction of a chemical potential-composition ( $\mu$ - $X$ ) diagram in the Ge- $\text{N}_2$  system (Figure 7). We recently found construction of such relationships to be useful for understanding formation of icosahedral  $\text{B}_6\text{O}_{1-x}$  phases within the B-O system at high pressures; such diagrams were developed by Darken and Gurry for understanding  $\text{Fe}_{1-x}\text{O}$  formation.<sup>55–57</sup> We assumed that only a single compound is formed within the Ge-N system, with an ideal composition  $\text{Ge}_3\text{N}_4$ . That compound is stable with respect to the

(55) Darken, L. S.; Gurry, R. W. *J. Am. Chem. Soc.* **1945**, *67*, 1398–1412.

(56) Gaskell, D. R. *Introduction to Thermodynamics of Materials*, 4th ed.; Taylor & Francis: New York, 2003.

(57) Darken, L. S.; Gurry, R. W. *J. Am. Chem. Soc.* **1946**, *68*, 798–819.



elements; that is, it has a lower free energy than the sum of  $3\text{Ge} + 2\text{N}_2$  (i.e., reaction 2). It is expected that some small dissolution occurs of  $\text{N}_2$  in Ge, and Ge in  $\text{N}_2$  fluid, described by appropriate Henry's law constants, and resulting in parabolic  $\mu-X$  relationships among the pure components. The composition of the  $\text{Ge}_3\text{N}_{4\pm x}$  phase is determined by common tangents with the elemental components with which it is in equilibrium (Figure 7). In our high  $P$ - $T$  experiments, the  $\text{N}_2$  component is always in excess. The intercept of the  $\text{Ge}_3\text{N}_{4-x}$ - $\text{N}_2$  common tangent with the pure  $\text{N}_2$  axis then determines the activity of that component in both phases. Because high  $P$ - $T$   $\text{N}_2$  is a fluid, its chemical potential decreases more rapidly than that of solid phases within the system as a function of  $T$  at constant  $P$  (due to the  $\text{N}_2$   $V(P, T)$  relations, expressed by its fugacity), and so the intercept of the common tangent with the  $\mu-X$  parabola for the  $\text{Ge}_3\text{N}_{4-x}$  phase moves to a more N-deficient composition (i.e., with larger  $x$ ) (Figure 7). In the Raman spectra shown in Figure 5, the relative intensity of the "defect doublet" changes by a factor of 2 between 2500 and 1700 K, which could be consistent with a compositional change between  $\text{Ge}_3\text{N}_{3.95}$  and  $\text{Ge}_3\text{N}_{3.85}$ , for example, as a function of temperature at  $P = 20$  GPa.

In future work, we will establish quantitative relationships between N vacancy concentrations and the relative intensity of defect-related Raman peaks at various synthesis pressures and temperatures. If we can confirm that the "extra" Raman peaks are indeed related to the presence of  $\text{N}^{3-}$  vacancy defects within the Ge- (and Si-; see below) nitride spinels, then this technique will provide a simple and rapid means for measurement and control of the chemical composition within the solid nitride spinel phases synthesized within the DAC at high pressures and high temperatures. That degree of compositional control is currently lacking in high  $P$ - $T$  solid-state/materials synthesis.<sup>19,58-61</sup>

In the case of the silicon nitride ( $\gamma\text{-Si}_3\text{N}_4$ ) spinel, very weak additional features were also noted to occur in the high-frequency  $\text{SiN}_4$  stretching region for samples recovered following synthesis under high  $P$ - $T$  conditions, which were not predicted by symmetry analysis. There was also an unexplained weak feature occurring in the spectra at  $\sim 560$   $\text{cm}^{-1}$  (Figure 4). In the spectra of samples synthesized from  $\text{Si} + \text{N}_2$  in the DAC at very high temperatures (i.e.,  $T > 2500$  K), these "extra" features became much more pronounced. Additional features were also observed to occur in the Raman spectra at  $\sim 750$   $\text{cm}^{-1}$ , and in the  $300$ - $450$   $\text{cm}^{-1}$  region (Figure 8). The relative intensities of these "additional" features to the  $\gamma\text{-Si}_3\text{N}_4$  spectrum all depend in a similar way upon the synthesis temperature and pressure, so that they likely corresponded to the formation of a single phase, or to the creation of "defects" within the spinel-structured compound.

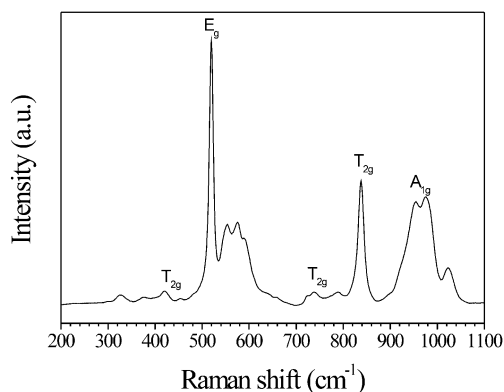


**Figure 8.** Raman spectra of  $\gamma\text{-Si}_3\text{N}_4$  at room pressure after laser-heating synthesis in the diamond anvil cell at 20 GPa and very high  $T$  (3000 K). The spectra display additional strong features around  $550$ - $600$  and  $900$ - $1050$   $\text{cm}^{-1}$ . Those features are proposed to be associated with the presence of  $\text{N}^{3-}$  vacancies in the sample.

The "additional" Raman peaks observed for  $\text{Si}_3\text{N}_4$  cannot be readily assigned to any of the expected Raman-active modes of other  $\text{Si}_3\text{N}_4$  phases that have been predicted to occur (but not yet observed).<sup>16,62</sup> For example, Kroll<sup>16</sup> calculated that a predicted high-density metastable willemite-II structured form should have a single Raman-active mode at  $690$   $\text{cm}^{-1}$ : although this could explain the occurrence of an "extra" high-frequency feature, it would be difficult to reconcile with the appearance of multiple peaks observed in the  $500$ - $600$   $\text{cm}^{-1}$  region (Figure 8). Here, we suggest instead that the additional Raman features could be assigned to Si-N stretching/bending vibrations of  $\text{SiN}_3$  units, associated with the formation of  $\text{N}^{3-}$  vacancies within the  $\gamma\text{-Si}_3\text{N}_4$  spinel structure, as we have proposed for  $\gamma\text{-Ge}_3\text{N}_4$ .

## Conclusion

We have obtained Raman spectra for  $\gamma\text{-Si}_3\text{N}_4$  and  $\gamma\text{-Ge}_3\text{N}_4$  spinels, obtained by high-pressure-high-temperature synthesis in the laser-heated diamond anvil cell, and also in multi-anvil high  $P$ - $T$  devices. We have assigned most of the expected Raman-active peaks predicted by theory, although several weaker modes that give rise to Raman-active vibrations still remain to be identified. We describe the appearance of "impurity" features that are due to micro- or nanocrystalline elemental Ge in some of the  $\gamma\text{-Ge}_3\text{N}_4$  samples. In spectra obtained from  $\gamma\text{-Ge}_3\text{N}_4$  samples synthesized under high  $P$ - $T$  conditions, additional modes occur in the high-frequency  $\text{GeN}_4$  stretching region that are not predicted by symmetry analysis. Here, we assign these features to the occurrence of N vacancies within the spinel structure, that is, associated with nonstoichiometric nitride spinels such as  $\gamma\text{-Ge}_3\text{N}_{4-x}$ . The N-defect concentration is adjusted by varying the synthesis conditions, in the presence of the  $\text{N}_2$  fluid medium, or by postsynthesis annealing procedures. We also observe similar "extra" Si-N stretching and bending features in the spectra of  $\gamma\text{-Si}_3\text{N}_4$  spinels synthesized at very high temperatures. We suggest that these are likewise due to the presence of  $\text{N}^{3-}$  vacancies within the  $\gamma\text{-Si}_3\text{N}_4$

(58) McMillan, P. F. In *International School of Physics "Enrico Fermi" Course CXLVII: High-Pressure Phenomena*; Hemley, R. J., Chiarotti, G. L., Bernasconi, M., Ulivi, L., Eds.; IOS Press: Amsterdam, Varenna on Como Lake, 2001; pp 477-507.

(59) McMillan, P. F. *High-Pressure Res.* **2004**, in press.

(60) McMillan, P. F. *High-Pressure Res.* **2003**, *23*, 7-22.

(61) McMillan, P. F. In *"High Pressure Phenomena"*, *Proc. Int. School of Physics "Enrico Fermi", Course CXLVII*; Hemley, R. J., Chiarotti, G. L., Bernasconi, M., Ulivi, L., Eds.; IOS Press: Amsterdam, pp 477-507.

(62) Soignard, E.; McMillan, P. F. **2004**, in preparation.

spinel structure. The results indicate that it may be possible to control and measure defect chemistries within group 14 nitride spinels synthesized under high  $P$ - $T$  conditions, by suitable control of the  $N_2$  activity, using Raman spectroscopy to establish and measure the  $\gamma$ -(Ge/Si) $_3$ N $_{4-x}$  stoichiometry in situ. This work will be important for future control over the optical and mechanical properties of this new family of solid-state materials.

**Acknowledgment.** This study was supported by EPSRC grant GR-R65206 to P.F.M. P.F.M. is a Wolfson Foundation-Royal Society Research Merit Award Fellow. We thank K. Leinenweber (Arizona State University) for advice and assistance during high-pressure-high-temperature multi-anvil synthesis of Si-Ge nitride samples.

CM049797+